Highly Sensitive Polymer Micro-Mesh for Measurement of Vacuum Packaged MEMS Devices

Manu Garg[1], Dhairya S. Arya[1], Mohamad G. Moinuddin[2], Satinder K. Sharma[2], Pushpapraj Singh[1]

[1]*Centre for Applied Research in Electronics (CARE), Indian Institute of Technology Delhi, New Delhi 110016, India*

[2]*Centre for Design & Fabrication of Electronic Devices, Indian Institute of Technology Mandi, Himachal Pradesh 175075, India*

Email: prsingh@care.iitd.ac.in

***Abstract*—The paper presents a polymer (SU-8) based MEMS Pirani gauge for the estimation of vacuum levels in packaged MEMS devices. The lower thermal conductivity of SU-8 (~0.2 W/m.K) offers enhanced sensitivity without incurring extra power consumption. Moreover, the micro-mesh structure offers effective coupling of ambient air/gas with the heated membrane resulting in improved thermal losses. Finite-Element-Model (FEM) analysis of the mesh are carried out using COMSOL Multiphysics®. A prototype structure is fabricated using a 3D lithographic technique to check the practicality of the idea. The simulation results show that the device can be used to measure vacuum levels from 4 Pa to 10E4 Pa. The linear range sensitivity of the simulated device is ~2.35 × 10E2 °C/mW/decade-Pa.**

Keywords—Pirani Gauge, MEMS, Thermal Conductivity, Vacuum Packaging.

I. Introduction

Micromachined Pirani gauges are being successfully deployed for in-situ vacuum characterization of rough to medium vacuum. The ability to detect in-package vacuum in real-time with high precision and reliability makes them a prominent choice over their conventional counterparts such as helium leak test and Q-factor extraction techniques [1-5]. Additionally, the heterogeneous integration offers seamless calibration of microsensor output over time.

State-of-the-art Pirani gauges consist of meander shaped silicon microbridge with multiple heat sinks to increase sensitivity and dynamic range [6-8]. The realization of the structure involves expensive etching techniques like Deep-Reactive-Ion Etching (DRIE) and wafer bonding. It increases the overall implementation cost of the device. Also, carbon nanotube and graphene-based Pirani gauge with extremely low footprints have been reported [9-10]. However, the synthesis of the sensing material is tedious. Membrane-based Pirani gauges offer broad range sensing, simplicity in architecture, CMOS compatibility, and ease of fabrication. Earlier reported membrane structures suffer from buckling and realization of nanogaps [11]. Over the years, several approaches have been proposed to increase dynamic range, sensitivity, and decreasing power consumption [6, 9, 12]. These authors reported scaling laws to achieve enhanced joule heating by increasing the length of the resistor while decreasing width and thickness. Similarly, multi heat sink based structures offer multiple paths for heat loss due to gaseous conduction. Apart from dimensional and structural engineering, physics plays an equally important role in determining the performance of MEMS-based Pirani gauges. Carefully reviewing the device physics reveals Pirani gauges operate in a transitional regime where the thermal conductivity of gas proportionally varies with pressure Neglecting radiation losses (Q_{rad}), the bottleneck of the minimum detectable pressure relies on solid losses. Heat loss via solid (Q_{solid}) can be given by Fourier's law as follows:

$$Q_{solid} = \frac{\lambda_{h,mat} . w . z}{l} \Delta T \quad (1)$$

Where, $\lambda_{h,mat}$ is the effective thermal conductivity of the sensing material, w is the width of the sensing material, z is the thickness of the sensing material, l is the length of the heater and ΔT is the average temperature increase. Eminently, lower thermal conductivity material and longer resistor with lowered width and thickness will minimize solid losses and ultimately lower limit of pressure detection. . A typical thermal conductivity vs pressure curve is shown in Fig. 1.

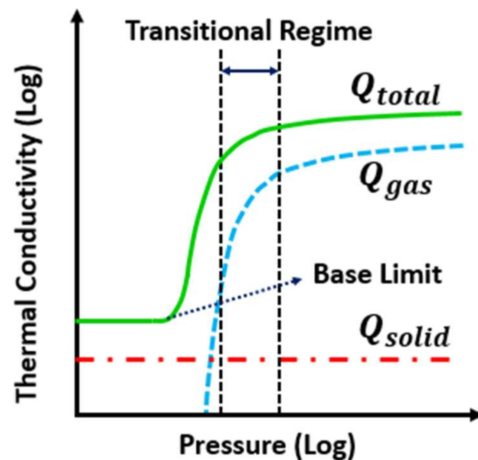

Figure 1: A typical thermal conductivity vs pressure curve highlighting the heat loss curves, transitional regime and base limit of vacuum detection.

In this paper, we propose a SU-8 micro-mesh-based Pirani gauge for vacuum characterization of packaged MEMS devices. The extremely low thermal conductivity (~0.2 W/m.K) of SU-8 decreases Q_{solid} and lower limit of the gauge. Moreover, the heat will be dissipated very slowly, thereby increasing sensitivity without incurring extra power consumption. This makes SU-8 a promising dielectric material for Pirani gauge applications.

II. Design & Description

Fig. 2 shows the schematic of a Pirani gauge for characterizing the vacuum of packaged MEMS devices. The device utilizes the suspended micro-heater heated by constant current/voltage bias. In constant current bias mode, a constant

978-1-7281-8660-3/20/$31.00 ©2020 IEEE

2020 5th IEEE International Conference on Emerging Electronics (ICEE) | 978-1-7281-8660-3/20/$31.00 ©2020 IEEE | DOI: 10.1109/ICEE50728.2020.9776980

Authorized licensed use limited to: Indian Institute Of Technology (IIT) Mandi. Downloaded on July 31,2024 at 08:26:34 UTC from IEEE Xplore. Restrictions apply.

current bias is applied at T_1 and T_2. As a result, the membrane heats up due to the Joule Heating phenomenon causing the output resistance (R_P) to change in reference to the average temperature increase. Mathematically, it can be given as:

$$R_P = R_o\big(1 + \alpha(\Delta T)\big) \quad (2)$$

where, R_0 is the nominal resistance of the platinum film at T_{ref} =293.15 K and α is the temperature coefficient of resistance. The average temperature of the mesh depends on the ambient pressure, thus reflecting the pressure variations at the output resistance (Eq. 7). Considering the 1D analytical model presented in [13], the heat balance equation can be given as:

$$\frac{\partial^2 t(x)}{\partial x^2} + \delta - \varepsilon t(x) = 0 \quad (3)$$

$$\delta = \frac{I^2 R_0}{\lambda_{h,mat}.\, w.\, l.\, z} \quad (4)$$

$$\varepsilon = \frac{\eta \lambda_{gas}(P)}{\lambda_{h,mat}.\, g.\, z} \quad (5)$$

where, $t(x)$ is the temperature distribution across the heated mesh, δ is the ohmic heat generation, ε is the pressure-dependent heat loss, I is the applied current bias, η is the correction factor incorporating fringing heat flux, $\lambda_{gas}(P)$ is the pressure-dependent thermal conductivity of gas, and g is the suspended gap.

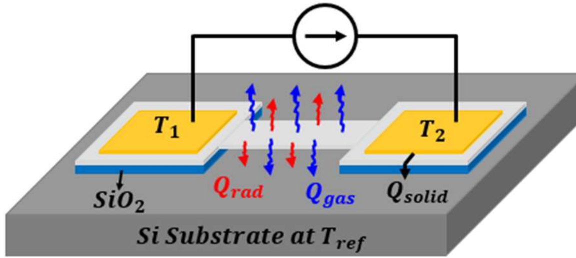

Figure 2: Schematic of Pirani gauge biased in constant current mode indicating the associated heat loss mechanisms.

Solving differential Eq. 3, the average increase in temperature (ΔT) across the membrane is given as:

$$\Delta T = \frac{\delta}{\varepsilon}\left(1 - \frac{tanh\left(\frac{\sqrt{\varepsilon}l}{2}\right)}{\left(\frac{\sqrt{\varepsilon}l}{2}\right)}\right) \quad (6)$$

And the corresponding output resistance can be calculated as:

$$R_p = R_o\left(1 + \frac{\alpha.\delta}{\varepsilon}\left(1 - \frac{tanh\left(\frac{\sqrt{\varepsilon}l}{2}\right)}{\left(\frac{\sqrt{\varepsilon}l}{2}\right)}\right)\right) \quad (7)$$

III. Fabrication of Polymer Micro-mesh

The prototype micro-mesh structure is fabricated using the grayscale lithography technique. The grayscale is created by changing the state of the mirrors that make up the DMD, between reflection and no-reflection at a specific frequency. This in turn will partially expose the resist making 3-dimensional structures possible [14]. The mask design is shown in Fig. 3. Initially, the SU-8 photoresist is spin-coated over the bare-Si sample. The second and most critical step is to variably expose the photoresist as per the mask shown in Fig. 3. As shown in Fig. 1(a), the UV light is exposed with full intensity at the anchor points and partially (Luminance Intensity ~130) where suspended beams are required. The sample is then post baked at 110 °C to promote cross-linkage and developed to remove photoresist from unexposed areas. A thin layer of Polymethyl methacrylate (PMMA) is then drop casted at the edge of the sample till it spreads over the entire sample. Afterward, a 100 nm of platinum is evaporated using e-beam evaporation. Finally, the PMMA is removed using acetone, thus lifting the platinum from unwanted areas. The complete fabrication steps are discussed in Fig. 4 and the SEM image of the fabricated device is shown in Fig. 5.

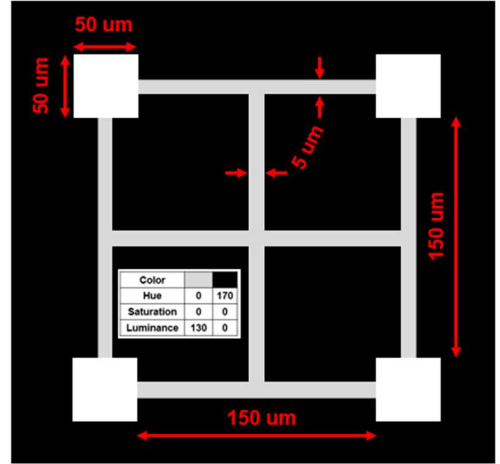

Color		
Hue	0	170
Saturation	0	0
Luminance	130	0

Figure 3: Grayscale mask for realizing the micro-mesh.

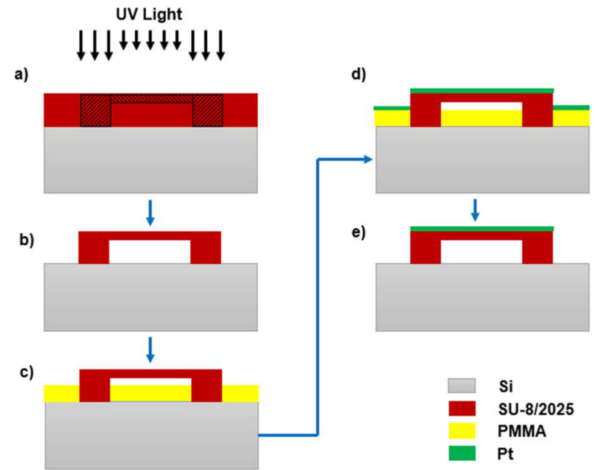

Figure 4: (a) Variable UV light exposure using maskless lithography system showing fully and partially exposed areas, (b) Post-bake treatment at 110 °C and development of photoresist, (c) PMMA drop casting, (d) E-beam evaporation of Platinum over the entire sample, (e) PMMA Lift-off using acetone.

Authorized licensed use limited to: Indian Institute Of Technology (IIT) Mandi. Downloaded on July 31,2024 at 08:26:34 UTC from IEEE Xplore. Restrictions apply.

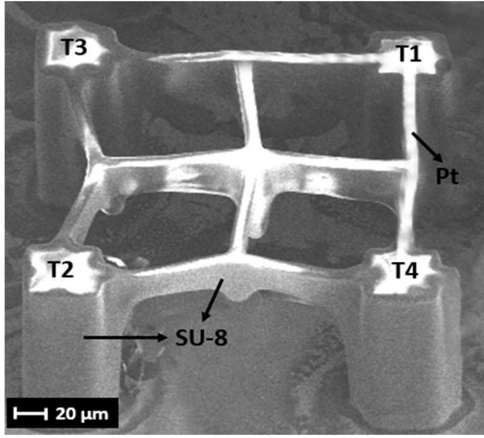

Figure 5: SEM image of the fabricated micro-mesh utilizing SU-8 as the heating membrane and platinum as the heater. The structure fabrication is one masked using maskless lithography technique.

IV. Results and Discussion

The electrothermal FEM analysis of the micro-mesh was carried using COMSOL Multiphysics®. The base of the substrate is set at T_{ref}, as the boundary condition. Also, the Multiphysics coupling between heat transfer and the AC/DC module was done to demonstrate the effect of Joule heating on the conduction through micro-heater. Further, the pressure-dependent environment is created by sealing the device in the air cavity whose thermal conductivity depends on the pressure inside the cavity. Fig. 6 shows the simulated response of the Micro-Mesh MEMS Pirani gauge with an embedded platinum heating element. The membrane is probed in a 4-point configuration driven by a constant current source at T_1, T_2 while measuring the voltage drop at T_3, T_4. The analysis reveals a uniform membrane temperature of 190 °C at the center of the membrane while decreasing to T_{ref} at anchor points.

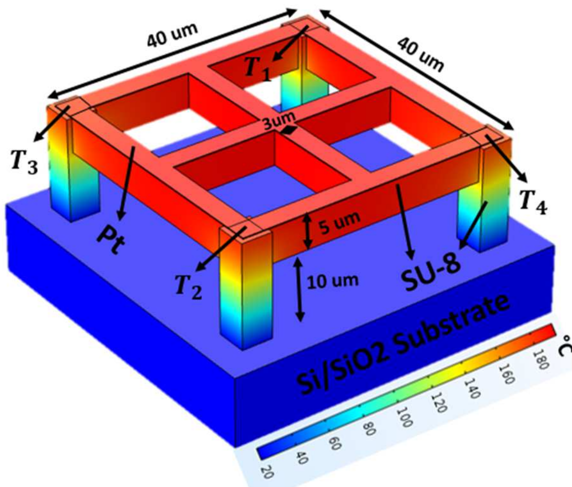

Figure 6: Simulated temperature profile of SU-8 membrane at 0.1 Pa biased at 56 µW.

The linear curves shown in Fig. 7 depicts the average temperature of the membrane for various applied input power at a constant ambient pressure. The slope of each linear curve gives the thermal impedance of the gauge for a typical value of pressure. Further, it also shows that for a typical value of pressure, the thermal impedance is constant. The thermal impedance vs pressure curve from 4 Pa to 10^4 Pa is shown in Fig. 8. The gauge has a sensitivity of 2.35×10^2 °C/mW/decade Pa and the minimum measurable vacuum level is 4 Pa.

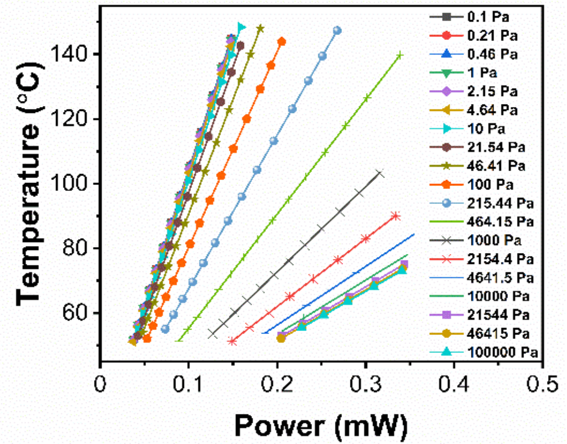

Figure 7: Simulated temperature variation of the gauge with the applied input power at different pressures.

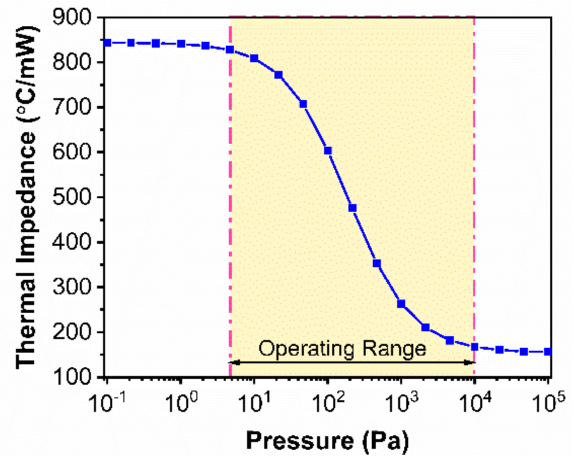

Figure 8: Simulated thermal impedance vs pressure curve highlighting the linear region with average sensitivity of 2.35×10^2 °C/mW/decade Pa

Conclusions

The polymer-based micro-mesh structure is simulated and a prototype structure is fabricated using massless lithography. The fabrication of the dsevice is quite cheap, simpler and only single lithography is required. The extracted sensitivity of the device is 2.35×10^2 °C/mW/decade Pa and the operating range of the device is 4 Pa to 10^4. Furthermore, using SU-8 as a dielectric membrane gives enhanced sensitivity without incurring extra power consumption.

Acknowledgment

The authors would like to acknowledge the Centre for Design and Fabrication of Electronic Devices (C4DFED) at IIT Mandi, Nanoscale Research Facility (NRF), and Central Research Facility (CRF) at Indian Institute of Technology New Delhi, India-110016.

References

[1] Chen, Y.C., Lin, W.C., Wang, H.S., Fan, C.C., Lin, K.C.H., Chou, B.C. and Liu, M.C.M., 2015, January. Differential micro-Pirani gauge for monitoring MEMS wafer-level package. In *2015 28th IEEE*

Authorized licensed use limited to: Indian Institute Of Technology (IIT) Mandi. Downloaded on July 31,2024 at 08:26:34 UTC from IEEE Xplore. Restrictions apply.

International Conference on Micro Electro Mechanical Systems (MEMS) (pp. 89-92). IEEE.

[2] Cheng, S.W., Weng, J.C., Hsu, H.C., Sun, Y.C., Chen, Y.C. and Fang, W., 2015, November. Modulate the chamber pressure of the hermetic sealed MEMS device by varying the cavity depth of cap Si. In *2015 IEEE SENSORS* (pp. 1-4). IEEE.

[3] Cheng, C.W., Chu, C.H., Hung, L.M. and Fang, W., 2017, June. 12 inch MEMS process for sensors implementation and integration. In *2017 19th International Conference on Solid-State Sensors, Actuators and Microsystems (TRANSDUCERS)* (pp. 402-405). IEEE.

[4] Liang, K.C., Cheng, C.W., Lin, C.H. and Fang, W., 2012, October. A novel low pressure sensor with fin-structures. In *SENSORS, 2012 IEEE* (pp. 1-4). IEEE.

[5] Wang, X., Liu, C., Zhang, Z., Liu, S. and Luo, X., 2010. A micro-machined Pirani gauge for vacuum measurement of ultra-small sized vacuum packaging. *Sensors and Actuators A: Physical*, *161*(1-2), pp.108-113.

[6] Kong, Y., Jiao, B., Zhang, L., Yun, S. and Chen, D., 2017, June. Design and fabrication of wafer-level packaged MEMS Pirani gauge with sorrounded heat sinks. In *2017 19th International Conference on Solid-State Sensors, Actuators and Microsystems (TRANSDUCERS)* (pp. 950-953). IEEE.

[7] Zhang, L.M., Jiao, B.B., Yun, S.C., Kong, Y.M. and Chen, D.P., 2017. Investigation and optimization of Pirani vacuum gauges with monocrystal silicon heaters and heat sinks. *Journal of Microelectromechanical Systems*, *26*(3), pp.601-608.

[8] Lai, J., Kong, Y., Jiao, B., Ye, Y., Yun, S., Liu, R., Ye, M. and Zhang, G., 2019. Study on Fusion Mechanisms for Sensitivity Improvement and Measurable Pressure Limit Extension of Pirani Vacuum Gauges With Multi Heat Sinks. *Journal of Microelectromechanical Systems*, *29*(1), pp.100-108.

[9] Yu, F. and Zhang, J., 2013. Single-walled Carbon nanotube pirani gauges prepared by DEP assembly. *IEEE transactions on nanotechnology*, *12*(3), pp.323-329.

[10] Romijn, J., Vollebregt, S., Dolleman, R.J., Singh, M., van der Zant, H.S., Steeneken, P.G. and Sarro, P.M., 2018, April. A miniaturized low power Pirani pressure sensor based on suspended graphene. In *2018 IEEE 13th Annual International Conference on Nano/Micro Engineered and Molecular Systems (NEMS)* (pp. 11-14). IEEE.

[11] Zhang, J., Jiang, W., Zhou, J. and Wang, X., 2009, June. A simple micro pirani vasuum gauge fabricated by bulk micromachining technology. In *TRANSDUCERS 2009-2009 International Solid-State Sensors, Actuators and Microsystems Conference* (pp. 280-283). IEEE.

[12] Jiang, W., Zhou, J., Wang, X., Wang, L. and Zhang, J., 2010, January. Fully coupled electro-thermal simulation of a micro pirani gauge. In *2010 IEEE 5th International Conference on Nano/Micro Engineered and Molecular Systems* (pp. 1088-1091). IEEE.

[13] Mastrangelo, C.H. and Muller, R.S., 1991. Microfabricated thermal absolute-pressure sensor with on-chip digital front-end processor. *IEEE journal of solid-state circuits*, *26*(12), pp.1998-2007.

[14] Madou, M.J., 2018. *Fundamentals of microfabrication: the science of miniaturization*. CRC press.

Authorized licensed use limited to: Indian Institute Of Technology (IIT) Mandi. Downloaded on July 31,2024 at 08:26:34 UTC from IEEE Xplore. Restrictions apply.